Sudan University of Science and Technology
College of Graduate Studies

Influence of Exposure Time of Nd: YAG Laser on Mechanical Properties and Particle Size of Zirconium Silicate

تأثير وقت التعرض لليزر Nd:YAG على الخواص الميكانيكية وحجم جزيئات سيليكات الزركونيوم

A Thesis Submitted as the Requirements for the Degree of Doctorate of Philosophy in Physics.

By:
Alaa Salah Aldin Awad Ala

Supervisor:

Ahmed Elhassan Elfaky

Co-Supervisor:
Dr.Ali Abdel Rahman Saeed Marouf

October 2020

الآيـــة

قال تعالى:

﴿ قَالَ يَٰقَوۡمِ أَرَءَيۡتُمۡ إِن كُنتُ عَلَىٰ بَيِّنَةٖ مِّن رَّبِّي وَرَزَقَنِي مِنۡهُ رِزۡقٗا حَسَنٗاۚ وَمَآ أُرِيدُ أَنۡ أُخَالِفَكُمۡ إِلَىٰ مَآ أَنۡهَىٰكُمۡ عَنۡهُۚ إِنۡ أُرِيدُ إِلَّا ٱلۡإِصۡلَٰحَ مَا ٱسۡتَطَعۡتُۚ وَمَا تَوۡفِيقِيٓ إِلَّا بِٱللَّهِۚ عَلَيۡهِ تَوَكَّلۡتُ وَإِلَيۡهِ أُنِيبُ ٨٨ ﴾

صدق الله العظيم

سورة هود/الآية: (88)

Dedication

I dedicate my dissertation work to my mother and my father for their patience and endless love.

I also dedicate this dissertation to my dear husband and to my dear sons.

I also dedicate this dissertation to my sister and without her encouragement; this work would not have seen the light.

My deepest thank goes to all my family and friends for helping me.

Acknowledgments

First of all, I would like to thanks Allah for giving me the strength to finish this study.

Special thanks Dr Ahmed Elhassan Elfaky supervisor of my dissertation for his guidance and assistance throughout the progress of this thesis, I would like to express my gratitude and thanks to Dr. Ali for his full assistance and complete supervision of this thesis and my thanks extend to staff of college of Science -Sudan University of Science and Technology.

Abstract

The surface modification obtained by laser beam irradiation requires a proper relationship among the laser beam parameters, to assure the irradiated surface morphology and physical chemistry properties surface. In this study, the photothermal effect of high power Nd: YAG laser at 1064 nm wavelength for different durations on the surface properties of zirconium silicate ($ZrSiO_4$) ceramics was investigated. Specimens of zirconium silicate ($ZrSiO_4$) ceramic pieces were divided into four samples according to irradiation duration as follows: one control sample (no treatment), and three samples irradiated with Nd: YAG laser at irradiation durations 3, 4 and 5 minutes. The irradiation was applied with fixed output power (60 W) with continuous mode. The samples hardness was measured, then SEM (Scanning Electron Microscope), EDX (Energy Dispersive X_ray), UV-visible spectroscopy and FTIR (Fourier Transform Inrared) characterization was done. The results show that high power Nd: YAG laser provide higher hardness surfaces compared to non-treated surface. SEM images demonstrate the formation of microstructures, smoother surface and solidification process occurring confirming the hardness results. FTIR spectra denotes the presence of quartz with small particle that improves mechanical strength of the zirconium silicate. Furthermore, EDX results reveal that laser irradiation does not change the chemical surface composition of ceramics. A linear correlation between laser irradiation duration and hardness, tensile strength and surface solidification was fond, without causing material defect.Moreover, Increase in transmittance of the irradiated zirconium silicate in the visible and near infrared range was also found using UV-vis spectroscopy.

المستخلص

يتطلب تعديل السطح الذي تم الحصول عليه عن طريق تشعيع شعاع الليزر علاقة مناسبة بين عوامل شعاع الليزر ، لضمان سطح التشكل وخصائص الكيمياء الفيزيائية. في هذه الدراسة ، تم فحص التأثير الحراري الضوئي لليزر الانديك عالي الطاقة عند طول موجة 1064 نانومتر لفترات مختلفة على خصائص سطح سيراميك سيليكات الزركونيوم ($ZrSiO_4$). عينات سيراميك سيليكات الزركونيوم ($ZrSiO_4$) هي: عينة تحكم واحدة (بدون علاج) ، وثلاث عينات مشعة بليزر الانديك في فترات التشعيع 3 و 4 و 5 دقائق. تم تطبيق التشعيع بقوة خرج ثابتة (60 واط) في الوضع المستمر. تم قياس صلابة العينات ، ثم تم إجراء التحليل الطيفي المرئي للأشعة فوق البنفسجية والتحليل الطيفي للاشعة تحت الحمراء وتحليل ال SEM و EDX . أظهرت النتائج أن ليزر الانديك عالي الطاقة يوفر أسطحًا أعلى صلابة مقارنة بالسطح غير المعالج. توضح صور SEM تكوين الهياكل المجهرية والسطح الأكثر سلاسة وعملية التصلب التي تؤكد نتائج الصلابة. تشير أطياف الاشعة تحت الحمراء إلى وجود الكوارتز بجزيئات صغيرة تعمل على تحسين القوة الميكانيكية لسيليكات الزركونيوم. علاوة على ذلك ، تكشف نتائج EDX أن تشعيع الليزر لا يغير التركيب الكيميائي للسطح للسيراميك. كان الارتباط الخطي بين مدة التشعيع بالليزر والصلابة وقوة الشد وتصلب السطح مغرمًا ، دون التسبب في عيب في المواد ، علاوة على ذلك ، تم العثور على زيادة في نفاذية سيليكات الزركونيوم المشع في نطاق الأشعة تحت الحمراء المرئي والقريب باستخدام التحليل الطيفي للأشعة فوق البنفسجية.

Table of Contents

List of Tables

List of Figures

CHAPTER ONE

INTRODUCTION

1.7. Background

Lasers have diverse applications in different fields such as medical, industrial, military and other different fields. In the industrial field lasers can used in many processes such as welding, cutting, drilling or surface solidifications. Laser-matter effects can be in diversified manners such as photothermal (represented by vaporization), ablation of matter (based on absorption) or in photochemical (direct breakage of chemical matter bonds).

Zirconia ceramic is a functional material and it has a leading position among ceramic materials. Its special properties, such as high mechanical strength, flexural resistance, make this ceramic material ideal for esthetic crowns, bridges, and frameworks in the anterior and posterior region (El-Ghany and Sherief, 2016).

1.8. Previous Studies

There have been numerous research studies the effect of laser matter irradiation; for example, on killing bacteria (laser milk pasteurization) (Marouf and Sara, 2018) (Amna and Marouf, 2018), silicon surface modification in solar cells (Marouf et al., 2014), food irradiation (bee honey irradiation) (Al Humira and Marouf, 2017) and production of highly value materials from agricultural waste

(Gawbah et al., 2017 and Gawbah et al., 2018). Other numerous researchs studies the interaction of low-level lasers with biological materials such as blood; for examples; investigating the effect of He-Ne laser on human whole blood (Haimid, et al., 2019 a) (Haimid, et al., 2019 b) and it also used to induce emission in human teeth to distinguish between dental caries and sound teeth (Marouf and Khairallah, 2019).

Meanwhile, ceramic materials in structural applications burned by large kilns to enhance its mechanical and surface properties. Also, different ceramic compositions are available for dental use, with varying properties that respond to different clinical indications. Now a days, the Nd:YAG laser has been suggested for employing to dental hard tissues for various usages, such as the effects of laser on surface morphology of dental restorative materials (Sanusi, et al., 2012)(Garcia-Sanz, et al., 2018), surface modification of Ti dental implants by laser (Braga, et al., 2014), laser treatment of dental ceramic/cement layers (Pich, et al., 2015), effects of laser on filling materials (Türkmen, et al., 2006) and effect of laser in hardness of dental ceramic (Ahmed, et al., 2014).

1.9. Research Problem

Different parameters like irradiated area, irradiation time, laser wavelength, pulse energy and the nature of the irradiated material determine largely the effect of the laser matter interaction. Besides, the surface modification obtained by laser beam

irradiation requires a proper relationship among the laser beam parameters, to assure the irradiated surface morphology and physical chemistry properties of surface. This study investigating the photo-thermal effect of high power Nd: YAG laser at 1064 nm wavelength for different durations on the surface properties of zirconium silicate ($ZrSiO_4$) ceramics.

1.10. The Objectives of this Dissertation

The aims of this study are to:

- Investigated the photo-thermal effect of high power Nd: YAG laser at 1064 nm wavelength for different durations on the surface properties of zirconium silicate ($ZrSiO_4$) ceramics.
- Identify the influence of high power Nd: YAG laser irradiation on the hardness and surface properties of zirconium silicate ($ZrSiO_4$) ceramics.
- Characterize the surface morphology of zirconium silicate following high power Nd: YAG laser irradiation.
- Determine the surface hardness of zirconium silicate following high power Nd: YAG laser irradiation.

1.11. Research Methodology

To achieve the objectives of this thesis, a commercial material will be brought and prepared through: grinding, sprayed, pressed, dried, and passed the glaze. Then the specimens will divided into four groups. Three of these groups will exposed by Nd: YAG laser (1064 nm wavelength) with 60 W output power at continuous mode, with different irradiation times and one specimen will left without treatment (A) as reference. After irradiation process, the specimens will be characterized.

1.12. Dissertation Layout

This dissertation is consist of four chapters, chapter one introduction and literature review, chapter two consist basic concepts of laser and ceramic and Laser-matter interaction**,** chapter three consist the experimental part (The materials and device and method), chapter four consist results and discussion, conclusion, and recommendations and finally list of references.

CHPTER TWO

BASIC CONCEPTS

2.1. Laser

The word laser is an acronym for light amplification by stimulated emission of radiation. Essentially a laser is an optical device that, when activated by an external energy source produces and emits a beam or pulse of monochromatic radiation in which all the waves are coherent and in phase. The emitted radiation is also highly collimated and directional in the sense that it is emitted as a narrow beam or pulse in a specific direction (Lytle et al., 1981).

In general terms, lasers are usually classified according to the type of material that is being used as the radiation source. The most common types are gas lasers, solid-state lasers, and semiconductor lasers. Other types that are used less frequently are liquid lasers, dye lasers, excimer lasers, etc. For the laser ranging, profiling, and scanning that is being carried out for topographic mapping purposes, where very high energy levels are required to perform distance measurements often over long ranges, only certain types of solid-state and semiconductor lasers have the very specific characteristics—high intensity combined with a high degree of collimation—that are necessary to carry out these operations (Petrie and Toth, 2008).

In lasers, as much as in discharge lamps, the light is emitted by atoms, ions or molecules that decay from a high to a low energy level. The peculiarity of lasers is that this transition is stimulated by photons identical, in all features, to those that the excited material would emit spontaneously to lose the excess energy (Figure 2.1). In other words, in the spontaneous emission process occurring in discharge lamps the excited atoms, ions or molecules release photons of different wavelengths and directions of propagation. In lasers, providing photons at one of these wavelengths and propagating at one specific direction ensures that the stimulated light will only be emitted at the same wavelength and along the same direction. This is the basic reason why the majority of lasers emit beam of monochromatic light

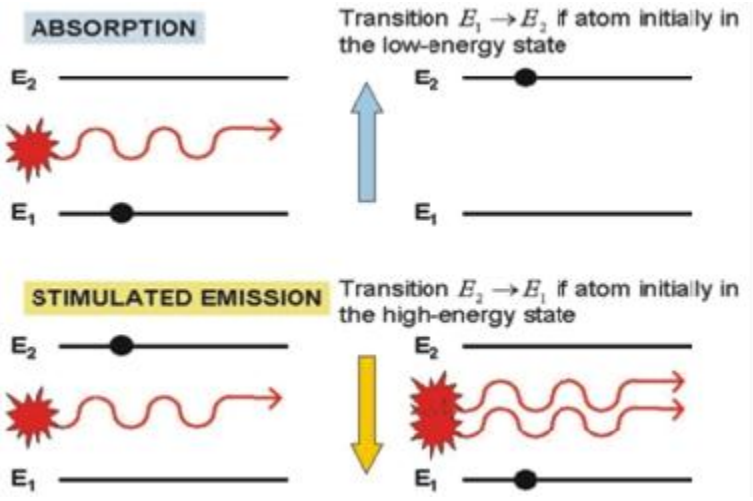

Figure 2.1: A photon with energy equal to E_2-E_1 can either disappear being absorbed by an atom initially in the state of energy E_1 (upper panel) or stimulated the emission of an identical photon by interacting with an atom initially in the state of energy E_2 (lower panel).

$$(E_2 - E_1) = \Delta E = h\,\upsilon \qquad (2.1)$$

where, h is the Planck's constant. This phenomenon is known as spontaneous emission. A spontaneously emitted photon may in turn excite another atom and stimulate it to emit a photon by de-exciting it to a lower energy level. This process is called stimulated emission of radiation.

Already at the beginning of the last century Plank and Einstein had discovered that the phenomenon of stimulated emission is the exact reverse of light absorption. In particular, as depicted in Figure 2.1, photons with energy equal to the difference between the energies of the excited and low levels of the material, $E_2 \rightarrow E_1$, have the same probability of being absorbed and promote the transition $E_1 \rightarrow E_2$ as of stimulating the emission of an identical photon and cause the decay $E_2 \rightarrow E_1$. Obviously, absorption diminishes the photon flux while stimulated emission increases it. If the latter phenomenon has to prevail, the majority of atoms, ions or molecules must be in the excited energy state rather than in the low-energy state, that is the photons must find the material in the situation that is called condition of population inversion (Figure 2.1).

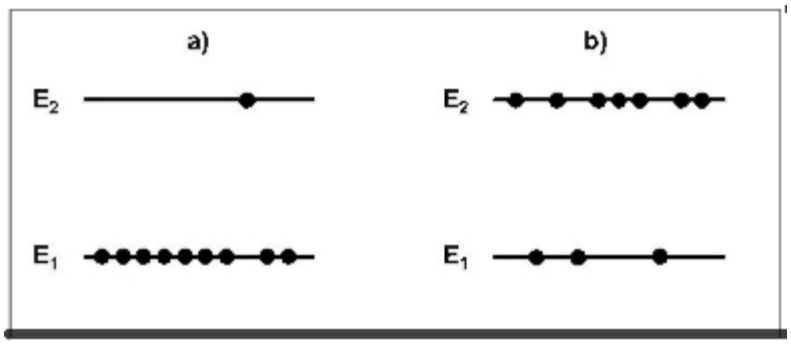

Figure 2.2: In general, the majority of atoms, ions or molecules occupy the low-energy state (a). In the condition of "population inversion" (b), the majority are in the high-energy state.

Since the population inversion depicted in Figure 2.2b corresponds to a rather unnatural situation, a strong source of excitation (pumping mechanism) is always present in a laser device to transform the material that would normally absorb light (Figure 2.2a), into one (active material) capable of amplifying light by stimulated emission. Gaseous active materials, such as N_2 molecules in the Nitrogen laser, mixtures of noble/halogen gases in the excimer lasers, Neon in the He-Ne laser or Ar+ in the Ar-ion laser, are pumped by electric currents; solid active materials like Nd+3 in the Yttrium Aluminum Garnet matrix (Nd: YAG laser) are optically pumped by either intense Xe-lamps or light-emitting diodes (Siegman, 1986).

2.1.1. Properties of laser

Laser radiation is characterized by an extremely high degree of monochromaticity, coherence, directionality, and brightness. We can add a fifth property, viz., short duration, which refers to the capability of producing very short light pulses, a less

fundamental but nevertheless very important property. We now consider these properties in some detail.

2.1.1.1 Monochromaticity

This property is due to the following two factors. First, only an EM wave of frequency $\upsilon_0 = (E_2-E_1)/h$ can be amplified, υ_0 has a certain range which is called line width, this line width is decided by homogeneous broadening factors and inhomogeneous broadening factors, the result line width is very small compared with normal lights. Second, the laser cavity forms a resonant system; oscillation can occur only at the resonance frequencies of this cavity. This leads to the further narrowing of the laser line width, the narrowing can be as large as 10 orders of magnitude! So laser light is usually very pure in wavelength, we say it has the property of monochromaticity.

2.1.1.2 Coherence

For any EM wave, there are two kinds of coherence, namely spatial and temporal coherence.

Let's consider two points that, at time t=0, lie on the same wave front of some given EM wave, the phase difference of EM wave at the two points at time t=0 is k0. If for any time t>0 the phase difference of EM wave at the two points remains k0, we say the EM wave has perfect coherence between the two points. If this is true for any two points of the wave front, we say the wave has perfect spatial

coherence. In practical the spatial coherence occurs only in a limited area, we say it is partial spatial coherence.

Now consider a fixed point on the EM wave front. If at any time the phase difference between time t and time t+dt remains the same, where "dt" is the time delay period, we say that the EM wave has temporal coherence over a time dt. If dt can be any value, we say the EM wave has perfect temporal coherence. If this happens only in a range $0<dt<t_0$, we say it has partial temporal coherence, with a coherence time equal to t_0.

We emphasize here that spatial and temporal coherence are independent. A partial temporal coherent wave can be perfect spatial coherent. Laser light is highly coherent, and this property has been widely used in measurement, holography, etc.

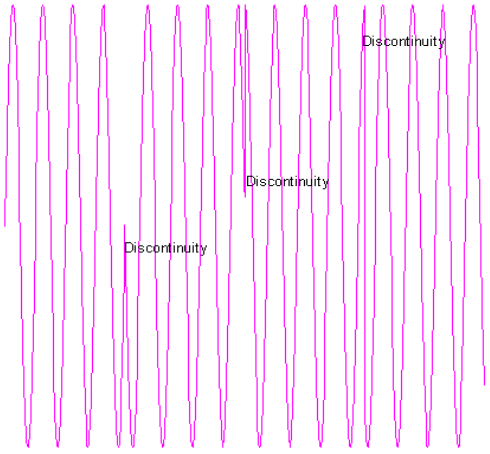

Figure 2.3: partial temporal coherence

2.1.1.3 Divergence and Directionality

Laser beam is highly directional, which implies laser light is of very small divergence. This is a direct consequence of the fact that laser beam comes from the resonant cavity, and only waves propagating along the optical axis can be sustained in the cavity. The directionality is described by the light beam divergence angle. Please try the figure below to see the relationship between divergence and optical systems.

For perfect spatial coherent light, a beam of aperture diameter D will have unavoidable divergence because of diffraction. From diffraction theory, the divergence angle θ_d is:

$$\theta_d = \beta \lambda / D \qquad (2.2)$$

Where λ and D are the wavelength and the diameter of the beam respectively, β is a coefficient whose value is around unity and depends on the type of light amplitude distribution and the definition of beam diameter. θ_d is called diffraction limited divergence.

If the beam is partial spatial coherent, its divergence is bigger than the diffraction limited divergence. In this case the divergence becomes:

$$\theta = \beta \lambda / (Sc)^{1/2} \qquad (2.3)$$

Where Sc is the coherence area.

2.1.1.4 Brightness

The brightness of a light source is defined as the power emitted per unit surface area per unit solid angle. A laser beam of power P, with a circular beam cross section of diameter D and a divergence angle q and the result emission solid angle is $\pi\ \theta^{2}$, then the brightness of laser beam is:

$$B=4P/(\pi D\theta)^{2} \qquad (2.4)$$

The max brightness is reached when the beam is perfect spatial coherent.

$$B_{max}=4P/(\pi\ \lambda\ \beta)^{2} \qquad (2.5)$$

In case of limited diffraction ($\theta_{d}=\lambda\ \beta\ /D$, $D=\lambda\ \beta\ /\theta_{d}$, $\theta_{d}=\theta$) (Renk, 2012).

2.1.2 Elements of Laser

All lasers comprise three main elements:

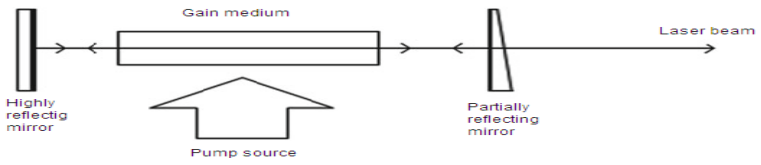

Figure 2.4: Schematic diagram of laser elements

1. The first of these elements comprises the active material of the laser that contains atoms whose electrons may be excited and raised to a much higher (metastable) energy level by an energy source. Examples of the materials that are being used extensively in the laser-based instruments that have been developed for the ranging, profiling, and scanning operations being carried out for topographic applications include a solid-state crystalline material such as neodymium-doped yttrium aluminum garnet (Nd:YAG) and a semiconductor material such as gallium arsenide (GaAs).

2. The second element that is present in every laser is an energy source. This provides the energy to start up and continue the lasing action. The continuous provision of energy to the laser is usually described as "pumping" the laser. Examples of suitable energy sources include optical sources such as a high-intensity discharge lamp or a laser diode, both of which are used with solid-state lasers. Alternatively, an electrical power unit producing a current that passes directly through the active material may be used as the energy source in the case of semiconductor lasers.

3. The third element is the provision of two mirrors: one that is fully reflective, reflecting 100% of the incident laser radiation; and the other that is semi-reflective (i.e., partly transmissive). Again these are integral components or features of every laser (Yariv, 1989).

2.1.3 Laser Types

This is a list of laser types, their operational wavelengths, and their applications. Thousands of kinds of laser are known, but most of them are used only for specialized research (Thys and Desmet, 2011).

2.1.3.1 Gas lasers

There are many of gas laser as shown in table 2.1

Table 2.1: Gas lasers

Laser gain Medium and type	Operation wavelength(s)	Pump source	Applications and notes
Helium–neon laser	632.8 nm (543.5 nm, 593.9 nm, 611.8 nm, 1.1523 μm, 1.52 μm, 3.3913 μm)	Electrical Discharge	Interferometry, holography, spectroscopy, barcode scanning, alignment, optical demonstrations.
Argon Laser	454.6 nm, 488.0 nm, 514.5 nm (351 nm, 363.8, 457.9 nm, 465.8 nm, 476.5 nm, 472.7 nm, 528.7 nm, also frequency doubled to provide 244 nm, 257 nm)	Electrical Discharge	Retinal phototherapy (for diabetes), lithography, confocal microscopy, spectroscopy pumping other lasers.
Krypton Laser	416 nm, 530.9 nm, 568.2 nm, 647.1 nm, 676.4 nm, 752.5 nm, 799.3 nm	Electrical Discharge	Scientific research, mixed with argon to create "white-light" lasers, light shows.
Xenon ion laser	Many lines throughout visible spectrum extending into the UV and IR.	Electrical Discharge	Scientific research
Nitrogen Laser	337.1 nm	Electrical Discharge	Pumping of dye lasers, measuring air pollution, scientific research. Nitrogen lasers can operate superradiantly (without a resonator cavity). Amateur laser

			construction. See TEA laser
Carbon dioxide laser	10.6 μm, (9.4 μm)	Transverse (highpower) Or longitudinal (lowpower) Electrical discharge	Material processing (laser cutting, laser beam welding, etc.), surgery, dental laser, military lasers.
Carbon monoxide laser	2.6 to 4 μm, 4.8 to 8.3 μm	Electrical Discharge	Material processing (engraving, welding, etc.), photoacoustic spectroscopy.
Excimer Laser	193 nm (ArF), 248 nm (KrF), 308 nm (XeCl), 353 nm (XeF)	Excimer recombination via electrical discharge	Ultraviolet lithography for semiconductor manufacturing, laser surgery, LASIK.

2.1.3.2 Chemical lasers

Used as directed-energy weapons, see table 2.2

Table 2.2: Chemical lasers

Laser gain medium and type	Operation wavelength(s)	Pump source	Applications and notes
Hydrogenfluoride laser	2.7 to 2.9 μ m for hydrogen fluoride (<80% atmospheric transmittance)	Chemical reaction in a burning jet of ethylene and nitrogen trifluoride (NF3)	Used in research for laser weaponry, operated in continuous wave mode, can have power in the megawatt range.
Deuterium fluoride laser	~3800 nm (3.6 to 4.2 μ m) (~90% atm. transmittance)	chemical reaction	US military laser prototypes.
COIL (Chemical oxygen-iodine laser)	1.315 μ m (<70% atmospheric transmittance)	Chemical reaction in a jet of singlet delta oxygen and iodine	Military lasers, scientific and materials research. Can operate in continuous wave mode, with power in the megawatt range.

Agil (All gasphase Iodine laser	1.315 μ m (<70% atmospheric transmittance)	Chemical reaction of chlorine atoms with gaseous hydrazoic acid, resulting in excited molecules of nitrogen chloride, which then pass their energy to the iodine atoms	Scientific, weaponry, aerospace

2.1.3.3 Dye lasers

The dye lasers as shown in table 2.3.

Table 2.3: Dye lasers

Laser gain medium and type	Operation wavelength(s)	Pump Source	Applications and notes
Dye lasers	390-435 nm (stilbene), 460-515 nm (coumarin 102), 570-640 nm (rhodamine 6G), many others	Other laser, flashlamp	Research,laser medicine,[2] spectroscopy, birthmark removal, isotope separation. The tuning range of the laser depends on which dye is used.

2.1.3.4 Solid-state lasers

There are many of Solid-state laser as shown in table 2.4

Table 2.4: Solid-state lasers

Laser gain medium and type	Operation wavelength(s)	Pump source	Applications and notes
Ruby laser	694.3 nm	Flashlamp	Holography, tattoo removal. The first type of visible light laser invented; May 1960.
Nd:YAG laser	1.064 μ m, (1.32 μ m)	Flashlamp, laser diode	Material processing, rangefinding, laser target designation, surgery, tattoo removal, hair removal, research, pumping other lasers (combined with frequency doubling to produce a green 532 nm beam). One of the most common high-power lasers. Usually pulsed (down to fractions of a nanosecond), dental laser
Nd:Cr:YAG laser	1.064 μ m, (1.32 μ m)	solar radiation	Experimental production of nanopowders.
Er:YAG laser	2.94 μ m	Flashlamp, laser diode	Periodontal scaling, dental laser, skin resurfacing
Neodymium YLF (Nd:YLF) solidstate laser	1.047 and 1.053 μ m	Flashlamp, laser diode	Mostly used for pulsed pumping of certain types of pulsed Ti:sapphire lasers, combined with frequency doubling.
Neodymiumdoped Yttrium orthovanadate (Nd:YVO4) laser	1.064 μ m	laser diode	Mostly used for continuous pumping of mode-locked Ti:sapphire or dye lasers, in combination with frequency doubling. Also used pulsed for marking and micromachining. A frequency doubled nd:YVO4 laser is also the normal way of making a green laser pointer.

Neodymium doped yttrium calcium oxoborate Nd:YCa4O(BO3)3 or simply Nd:YCOB	~1.060 μ m (~530 nm at second harmonic)	laser diode	Nd:YCOB is a so-called "self-frequency doubling" or SFD laser material which is both capable of lasing and which has nonlinear characteristics suitable for second harmonic generation. Such materials have the potential to simplify the design of high brightness green lasers.
Neodymium glass (Nd:Glass) laser	~1.062 μ m (silicate glasses), ~1.054 μ m (phosphate glasses)	Flashlamp, laser diode	Used in extremely high-power (terawatt scale), high-energy (megajoules) multiple beam systems for inertial confinement fusion. Nd:Glass lasers are usually frequency tripled to the third harmonic at 351 nm in laser fusion devices.
Ytterbium:2O3 (glass or ceramics) laser	1.03 μ m	Laser diode	Ultrashort pulse research,
Holmium YAG (Ho:YAG) laser	2.1 μ m	Laser diode	Tissue ablation, kidney stone removal, dentistry.
Thulium YAG (Tm:YAG) laser	2.0 μ m	Laser diode	LIDAR.
Erbium-doped and erbium‑ytterbium codoped glass lasers	1.53-1.56 μ m	Laser diode	These are made in rod, plate/chip, and optical fiber form. Erbium doped fibers are commonly used as optical amplifiers for telecommunications.
F-center laser.	2.3-3.3 μ m	Ion laser	Spectroscopy

2.1.3.5 Other types of lasers

There are many of Other types of laser as shown in table 2.5.

Table 2.5: Other types of lasers

Laser gain medium and type	Operation wavelength(s)	Pump source	Applications and notes
Free-electron laser	A broad wavelength range (0.1 nm - several mm); a single free electron laser may be tunable over a wavelength range	Relativistic electron beam	Atmospheric research, material science, medical applications.
Gas dynamic laser	Several lines around 10.5 μ m; other frequencies may be possible with different gas mixtures	Spin state population inversion in carbon dioxide	molecules caused by supersonic adiabatic expansion of mixture of nitrogen and carbon dioxide Military applications; can operate in CW mode at several megawatts optical power. Manufacturing and Heavy Industry.
"Nickel-like" samarium laser[10]	X-rays at 7.3 nm Wavelength	Lasing in ultra-hot samarium plasma formed by double pulse terawatt scale irradiation fluences.	Sub‑10 nm X-ray laser, possible applications in high-resolution microscopy and holography.

Raman laser, uses inelastic stimulated Raman scattering in a nonlinear media, mostly fiber, for amplification	1-2 μ m for fiber version	Other laser, mostly Yb-glass fiber Lasers	Complete 1-2 μ m wavelength coverage; distributed optical signal amplification for telecommunications; optical solitons generation and amplification
Nuclear pumped laser Research,	See gas lasers, soft x-ray	Nuclear fission: reactor, nuclear Bomb	weapons program.
Gamma-ray laser	Gamma rays	Unknown	Hypothetical
Gravity laser	Very long gravitational Waves	Unknown	Hypothetical

2.1.4 Laser Applications

Lasers can be used for welding, cladding, marking, surface treatment, drilling, and cutting among other manufacturing processes. It is used in the automobile, shipbuilding, aerospace, steel, electronics, and medical industries for precision machining of complex parts. Laser welding is advantageous in that it can weld at speeds of up to 100 mm/s as well as the ability to weld dissimilar metals. Laser cladding is used to coat cheap or weak parts with a harder material in order to improve the surface quality. Drilling and cutting with lasers is advantageous in that there is little to no wear on the cutting tool as there is no contact to cause damage. Milling with a laser is a three dimensional process that requires two lasers, but

drastically cuts costs of machining parts. Lasers can be used to change the surface properties of a workpiece. Cutting depth Applications the appliance of laser beam machining varies depending on the industry. In light manufacturing the machine is used to engrave and to drill other metals. In the electronic industry laser beam machining is used for wire stripping and skiving of circuits. In the medical industry it is used for cosmetic surgery and hair removal (Dubey and Yadava, 2008).

2.2 Ceramic

A ceramic material is an inorganic, non-metallic, often crystalline oxide, nitride or carbide material. Some elements, such as carbon or silicon, may be considered ceramics. Ceramic materials are brittle, hard, strong in compression, and weak in shearing and tension. They withstand chemical erosion that occurs in other materials subjected to acidic or caustic environments. Ceramics generally can withstand very high temperatures, ranging from 1,000 °C to 1,600 °C (1,800 °F to 3,000 °F). Glass is often not considered a ceramic because of its amorphous (non crystalline) character. However, glassmaking involves several steps of the ceramic process, and its mechanical properties are similar to ceramic materials.

Crystalline ceramic materials are not amenable to a great range of processing. Methods for dealing with them tend to fall into one of two categories – either makes the ceramic in the desired shape, by reaction in situ, or by "forming" powders into the desired shape, and then sintering to form a solid body. Ceramic

forming techniques include shaping by hand (sometimes including a rotation process called "throwing"), slip casting, tape casting (used for making very thin ceramic capacitors), injection molding, dry pressing, and other variations.

Non crystalline ceramics, being glass, tend to be formed from melts. The glass is shaped when either fully molten, by casting, or when in a state of toffee-like viscosity, by methods such as blowing into a mold. If later heat treatments cause this glass to become partly crystalline, the resulting material is known as a glass ceramic, widely used as cook-tops and also as a glass composite material for nuclear waste disposal (Seuba et al., 2016).

2.2.1 Properties of Ceramic

There are many properties of ceramic such as:

2.2.1.1 Mechanical Properties

Mechanical properties are important in structural and building materials as well as textile fabrics. In modern materials science, fracture mechanics is an important tool in improving the mechanical performance of materials and components. It applies the physics of stress and strain, in particular the theories of elasticity and plasticity, to the microscopic crystallographic defects found in real materials in order to predict the macroscopic mechanical failure of bodies. Fractography is widely used with fracture mechanics to understand the causes of failures and also verify the

theoretical failure predictions with real life failures. Ceramic materials are usually ionic or covalent bonded materials, and can be crystalline or amorphous. A material held together by either type of bond will tend to fracture before any plastic deformation takes place, which results in poor toughness in these materials. Additionally, because these materials tend to be porous, the pores and other microscopic imperfections act as stress concentrators, decreasing the toughness further, and reducing the tensile strength. These combine to give catastrophic failures, as opposed to the more ductile failure modes of metals (McColm, 2013).

2.2.1.2 Electrical properties

i. Semiconductors

Some ceramics are semiconductors. Most of these are transition metal oxides that are II-VI semiconductors, such as zinc oxide. While there are prospects of mass-producing blue LEDs from zinc oxide, ceramicists are most interested in the electrical properties that show grain boundary effects. One of the most widely used of these is the varistor. These are devices that exhibit the property that resistance drops sharply at a certain threshold voltage. Once the voltage across the device reaches the threshold, there is a breakdown of the electrical structure in the vicinity of the grain boundaries, which results in its electrical resistance dropping from several megohms down to a few hundred ohms. The major advantage of these is

that they can dissipate a lot of energy, and they self-reset – after the voltage across the device drops below the threshold, its resistance returns to being high.

ii. Superconductivity

Under some conditions, such as extremely low temperature, some ceramics exhibit high temperature superconductivity. The reason for this is not understood, but there are two major families of superconducting ceramics.

iii. Ferroelectricity and supersets

Piezoelectricity, a link between electrical and mechanical response, is exhibited by a large number of ceramic materials, including the quartz used to measure time in watches and other electronics. Such devices use both properties of piezoelectrics, using electricity to produce a mechanical motion (powering the device) and then using Electrical properties Semiconductors Superconductivity Ferroelectricity and supersets Silicon nitride rocket thruster. Left: Mounted in test stand. Right: Being tested with H_2/O_2 propellants Cermax xenon arc lamp with synthetic sapphire output window this mechanical motion to produce electricity (generating a signal). The unit of time measured is the natural interval required for electricity to be converted into mechanical energy and back again.

The piezoelectric effect is generally stronger in materials that also exhibit pyroelectricity, and all pyroelectric materials are also piezoelectric. These materials can be used to inter-convert between thermal, mechanical, or electrical energy; for

instance, after synthesis in a furnace, a pyroelectric crystal allowed to cool under no applied stress generally builds up a static charge of thousands of volts. Such materials are used in motion sensors, where the tiny rise in temperature from a warm body entering the room is enough to produce a measurable voltage in the crystal. In turn, pyroelectricity is seen most strongly in materials which also display the ferroelectric effect, in which a stable electric dipole can be oriented or reversed by applying an electrostatic field. Pyroelectricity is also a necessary consequence of ferroelectricity. This can be used to store information in ferroelectric capacitors, elements of ferroelectric RAM**.**

The most common such materials are lead zirconate titanate and barium titanate. Aside from the uses mentioned above, their strong piezoelectric response is exploited in the design of high-frequency loudspeakers, transducers for sonar, and actuators for atomic force and scanning tunneling microscopes.

iv. Positive thermal coefficient

Increases in temperature can cause grain boundaries to suddenly become insulating in some semiconducting ceramic materials, mostly mixtures of heavy metal titanates. The critical transition temperature can be adjusted over a wide range by variations in chemistry. In such materials, current will pass through the material until joule heating brings it to the transition temperature, at which point the circuit will be broken and current flow will cease. Such ceramics are used as self-

controlled heating elements in, for example, the rear-window defrosts circuits of automobiles. At the transition temperature, the material's dielectric response becomes theoretically infinite. While a lack of temperature control would rule out any practical use of the material near its critical temperature, the dielectric effect remains exceptionally strong even at much higher temperatures. Titanates with critical temperatures far below room temperature have become synonymous with "ceramic" in the context of ceramic capacitors for just this reason.

2.2.1.3 Optical properties

Optically transparent materials focus on the response of a material to incoming light waves of a range of wavelengths. Frequency selective optical filters can be utilized to alter or enhance the brightness and contrast of a digital image. Guided light wave transmission via frequency selective waveguides involves the emerging field of fiber optics and the ability of certain glassy compositions as a transmission medium for a range of frequencies simultaneously (multi-mode optical fiber) with little or no interference between competing wavelengths or frequencies. This resonant mode of energy and data transmission via electromagnetic (light) wave propagation, though low powered, is virtually lossless. Optical waveguides are used as components in integrated optical circuits (e.g. light-emitting diodes, LEDs) or as the transmission medium in local and long haul optical communication systems. Also of value to the emerging materials scientist is the sensitivity of materials to

radiation in the thermal infrared (IR) portion of the electromagnetic spectrum. This heat-seeking ability is responsible for such diverse optical phenomena as Night-vision and IR luminescence.

Thus, there is an increasing need in the military sector for high-strength, robust materials which have the capability to transmit light (electromagnetic waves) in the visible (0.4 – 0.7 micrometers) and mid-infrared (1 – 5 micrometers) regions of the spectrum. These materials are needed for applications requiring transparent armor, including next-generation high speed missiles and pods, as well as protection against improvised explosive devices (IED).

In the 1960s, scientists at General Electric (GE) discovered that under the right manufacturing conditions, some ceramics, especially aluminium oxide (alumina), could be made translucent. These translucent materials were transparent enough to be used for containing the electrical plasma generated in high-pressure sodium street lamps. During the past two decades, additional types of transparent ceramics have been developed for applications such as nose cones for heat-seeking missiles, windows for fighter aircraft, and scintillation counters for computed tomography scanners.

In the early 1970s, Thomas Soules pioneered computer modeling of light transmission through translucent ceramic alumina. His model showed that microscopic pores in ceramic, mainly trapped at the junctions of microcrystalline

grains, caused light to scatter and prevented true transparency. The volume fraction of these microscopic pores had to be less than 1% for high-quality optical transmission.

This is basically a particle size effect. Opacity results from the incoherent scattering of light at surfaces and interfaces. In addition to pores, most of the interfaces in a typical metal or ceramic object are in the form of grain boundaries which separate tiny regions of crystalline order. When the size of the scattering center (or grain boundary) is reduced below the size of the wavelength of the light being scattered, the scattering no longer occurs to any significant extent.

In the formation of polycrystalline materials (metals and ceramics) the size of the crystalline grains is determined largely by the size of the crystalline particles present in the raw material during formation (or pressing) of the object. Moreover, the size of the grain boundaries scales directly with particle size. Thus a reduction of the original particle size below the wavelength of visible light (~ 0.5 micrometers for shortwave violet) eliminates any light scattering, resulting in a transparent material.

Recently, Japanese scientists have developed techniques to produce ceramic parts that rival the transparency of traditional crystals (grown from a single seed) and exceed the fracture toughness of a single crystal. In particular, scientists at the

Japanese firm Konoshima Ltd., a producer of ceramic construction materials and industrial chemicals, have been looking for markets for their transparent ceramics. Livermore researchers realized that these ceramics might greatly benefit high-powered lasers used in the National Ignition Facility (NIF) Programs Directorate. In particular, a Livermore research team began to acquire advanced transparent ceramics from Konoshima to determine if they could meet the optical requirements needed for Livermore's Solid-State Heat Capacity Laser (SSHCL) (Radousky, 2006).

2.2.2 Examples

A composite material of ceramic and metal is known as cermet.

Other ceramic materials, generally requiring greater purity in their make-up than those above, include forms of several chemical compounds, including:

i. Barium titanate (often mixed with strontium titanate) displays ferroelectricity, meaning that its mechanical, electrical, and thermal responses are coupled to one another and also historydependent. It is widely used in electromechanical transducers, ceramic capacitors, and data storage elements. Grain boundary conditions can create PTC effects in heating elements.
ii. Bismuth strontium calcium copper oxide, a high-temperature superconductor

iii. Boron oxide is used in body armour. Boron nitride is structurally isoelectronic to carbon and takes on similar physical forms: a graphite-like one used as a lubricant, and a diamond-like one used as an abrasive.

iv. Earthenware used for domestic ware such as plates and mugs. Ferrite is used in the magnetic cores of electrical transformers and magnetic core memory.

v. Lead zirconate titanate (PZT) was developed at the United States National Bureau of Standards in 1954. PZT is used as an ultrasonic transducer, as its piezoelectric properties greatly exceed those of Rochelle salt (Wachtman, 2006).

vi. Magnesium diboride (MgB_2) is an unconventional superconductor.

vii. Porcelain is used for a wide range of household and industrial products.

viii. Sialon (Silicon Aluminium Oxynitride) has high strength; resistance to thermal shock, chemical and wear resistance, and low density. These ceramics are used in non-ferrous molten metal handling, weld pins and the chemical industry.

ix. Silicon carbide (SiC) is used as a susceptor in microwave furnaces, a commonly used abrasive, and as a refractory material.

x. Silicon nitride (Si_3N_4) is used as an abrasive powder.

xi. Steatite (magnesium silicates) is used as an electrical insulator. Titanium carbide Used in space shuttle re-entry shields and scratchproof watches.

xii. Uranium oxide (UO_2), used as fuel in nuclear reactors.

xiii. Yttrium barium copper oxide ($YBa_2Cu_3O_7-x$), another high temperature superconductor.

xiv. Zinc oxide (ZnO), which is a semiconductor, and used in the construction of varistors.

xv. Zirconium dioxide (zirconia), which in pure form undergoes many phase changes between room temperature and practical sintering temperatures, can be chemically "stabilized" in several different forms. Its high oxygen ion conductivity recommends it for use in fuel cells and automotive oxygen sensors. In another variant, metastable structures can impart transformation toughening for mechanical applications; most ceramic knife blades are made of this material.

xvi. Partially stabilised zirconia (PSZ) is much less brittle than other ceramics and is used for metal forming tools, valves and liners, abrasive slurries, kitchen knives and bearings subject to severe abrasion (Garvie et al., 1975).

2.2.3 Products

For convenience, ceramic products are usually divided into four main types; these are shown below with some examples:

i. Structural, including bricks, pipes, floor and roof tiles Refractories, such as kiln linings, gas fire radiants, steel and glass making crucibles

ii. Whitewares, including tableware, cookware, wall tiles, pottery products and sanitary ware (Geiger and Greg, 2018).

2.2.4 Ceramics made with clay

Frequently, the raw materials of modern ceramics do not include clays. Those that do are classified as follows:

i. Earthenware, fired at lower temperatures than other types

ii. Stoneware, vitreous or semi-vitreous

iii. Porcelain, which contains a high content of kaolin

iv. Bone china

2.2.5 Classification

Ceramics can also be classified into three distinct material categories:

i. Oxides: alumina, beryllia, ceria, zirconia

ii. Non-oxides: carbide, boride, nitride, silicide

iii. Composite materials: particulate reinforced, fiber reinforced, combinations of oxides and nonoxides.

Each one of these classes can be developed into unique material properties because ceramics tend to be crystalline.

2.2.6 Applications

i. Knife blades: the blade of a ceramic knife will stay sharp for much longer than that of a steel knife, although it is more brittle and susceptible to breaking.

ii. Carbon-ceramic brake disks for vehicles are resistant to brake fade at high temperatures.

iii. Advanced composite ceramic and metal matrices have been designed for most modern armoured fighting vehicles because they offer superior penetrating resistance against shaped charges (such as HEAT rounds) and kinetic energy penetrators.

iv. Ceramics such as alumina and boron carbide have been used in ballisti armored vests to repel high-velocity rifle fire. Such plates are known commonly as small arms protective inserts, or SAPIs. Similar material is used to protect the cockpits of some military airplanes, because of the low weight of the material.

v. Ceramics can be used in place of steel for ball bearings. Their higher hardness means they are much less susceptible to wear and typically last for triple the lifetime of a steel part. They also deform less under load, meaning they have less contact with the bearing retainer walls and can roll faster. In very high speed applications, heat from friction during rolling can cause problems for metal bearings, which are reduced by the use of ceramics. Ceramics are also more chemically resistant and can be used in wet environments where steel bearings would rust. In some cases, their electricity-insulating properties may also be valuable in bearings. Two drawbacks to ceramic bearings are a significantly higher cost and susceptibility to damage under shock loads.

vi. In the early 1980s, Toyota researched production of an adiabatic engine using ceramic components in the hot gas area. The ceramics would have allowed temperatures of over 3000 °F (1650 °C). The expected advantages would have been lighter materials and a smaller cooling system (or no need for one at all), leading to a major weight reduction. The expected increase of fuel efficiency of the engine (caused by the higher temperature, as shown by Carnot's theorem) could not be verified experimentally; it was found that the heat transfer on the hot ceramic cylinder walls was higher than the transfer to a cooler metal wall as the cooler gas film on the metal surface works as a thermal insulator. Thus, despite all of these desirable properties, such engines have not succeeded in production because of costs for the ceramic components and the limited advantages. (Small imperfections in the ceramic material with its low fracture toughness lead to cracks, which can lead to potentially dangerous equipment failure.) Such engines are possible in laboratory settings, but mass production is not feasible with current technology.

vii. Work is being done in developing ceramic parts for gas turbine engines. Currently, even blades made of advanced metal alloys used in the engines' hot section require cooling and careful limiting of operating temperatures. Turbine engines made with ceramics could operate more efficiently, giving aircraft greater range and payload for a set amount of fuel.

viii. Recent advances have been made in ceramics which include bioceramics, such as dental implants and synthetic bones. Hydroxyapatite, the natural mineral component of bone, has been made synthetically from a number of biological and chemical sources and can be formed into ceramic materials. Orthopedic implants coated with these materials bond readily to bone and other tissues in the body without rejection or inflammatory reactions so are of great interest for gene delivery and tissue engineering scaffolds. Most hydroxyapatite ceramics are very porous and lack mechanical strength, and are used to coat metal orthopedic devices to aid in forming a bond to bone or as bone fillers. They are also used as fillers for orthopedic plastic screws to aid in reducing the inflammation and increase absorption of these plastic materials. Work is being done to make strong, fully dense nanocrystalline hydroxyapatite ceramic materials for orthopedic weight bearing devices, replacing foreign metal and plastic orthopedic materials with a synthetic, but naturally occurring, bone mineral. Ultimately, these ceramic materials may be used as bone replacements or with the incorporation of protein collagens, synthetic bones.

ix. Durable actinide-containing ceramic materials have many applications such as in nuclear fuels for burning excess Pu and in chemically-inert sources of alpha irradiation for power supply of unmanned space vehicles or to produce electricity for microelectronic devices. Both use and disposal of radioactive actinides require

their immobilisation in a durable host material. Nuclear waste long-lived radionuclides such as actinides are immobilised using chemically-durable crystalline materials based on polycrystalline ceramics and large single crystals.

x. High-tech ceramic is used in watchmaking for producing watch cases. The material is valued by watchmakers for its light weight, scratch resistance, durability and smooth touch. IWC is one of the brands that initiated the use of ceramic in watchmaking (Lee et al., 2010).

2.3 Laser Matter Interaction

A good understanding of the phenomena that take place when laser radiation interacts with matter is a key element for the success and optimization of any laser-based application. In general, let us assume that radiation having fluence, that is, energy per unit area, F_o, interacts with a material. Part of the energy may be absorbed by the material (F_{ab}), part may be scattered (F_{sc}), and part may be transmitted (F_{tr}).

The overall energy balance is given by Equation (2.6):

$$F_0 = F_{ab} + F_{sc} + F_{tr} \quad (2.6)$$

In turn, the absorbed fluence F_{ab} may eventually cause thermal effects (F_{th}) or photochemical modifications (F_{ph}) in the material, and part of it may be reemitted as fluorescence or phosphorescence (F_{fl}). These processes are described by Equation (2.7):

$$F_{ab} = F_{th} + F_{ph} + F_{fl} \quad (2.7)$$

The values of the terms F_{sc}, F_{tr}, and F_{fl} may be used for obtaining diagnostic information for the identity and quantity of the material components. The interplay between the terms F_{sc} and F_{tr}, for example, is the basis for the imaging technique called reflectography, which depending on the wavelength of the incident radiation is either infrared (IR) or ultraviolet (UV) reflectography. Also, qualitative and quantitative analysis of the composition of a material may be obtained from the terms F_{tr} and F_{fl}. In contrast, F_{th} and F_{ph} may be exploited for material modifications and processing. For example, the cleaning or more generally the removal of unwanted materials from the surface of a target material may come about as the final consequence of such effects. The relative importance of the various terms involved in the above simplified scheme, which describes how radiation interacts with matter, may be controlled to a large extent when a laser is used as the radiation source. Effectively there are three important considerations, whose interplay determines the final outcome in this case. The laser parameters: wavelength, fluence (energy per unit area), intensity.

The laser parameters: wavelength, fluence (energy per unit area), intensity, pulse duration, pulse repetition rate, mode of operation (continuous or pulsed), beam quality, and coherence length.

The material parameters: absorption coefficient, heat capacity, thermal conductivity, and other physical properties.

The ambient environment: air, inert atmosphere, or vacuum. This is important for the presence of secondary effects following the interaction, for example, oxidation processes, which may influence the final outcome.

The appropriate combination of these parameters is critical for the success of any laser-based application. In the laser cleaning of artifacts, for example, depending on the nature of the materials to be removed (e.g., black encrustations, organic materials such as polymerized or oxidized varnish) and the underlying original surface (e.g., stonework, painted layer), it is crucial to define the optimal laser parameters so that the dirt or pollutants will be removed (ablated) while any thermal

or photochemical effects due to the absorbed laser radiation [Equation (2.7)] are confined as much as possible to the outermost layer occupied by these unwanted materials, without affecting the original underlying surface. As will be described later in this book, a viable option for the cleaning of polymerized or oxidized varnish layers from painted artworks is the use of pulsed lasers, which emit pulses of nanosecond duration at ultraviolet wavelengths ($\lambda < 250$ nm), which are strongly absorbed by these layers.

There are many processes and effects that may take place as a result of the interaction between laser light and a material. These are determined by the properties of the material and the laser parameters. Considering that to date a large number of laser sources is available and that each of them causes different effects depending on the parameters of its operation, the optimization of any specific application relies largely on the selection of the appropriate laser. Different types of laser sources that are employed in cultural heritage applications and the wavelengths.

Finally, it is not only the laser source but also the design and engineering of the overall workstation that will determine the degree of success of a laser application (Fotakis et al., 2006).

CHAPTER THREE

EXPERIMENTAL PART

3.1. Introduction

This chapter describes the experimental portion, including the preparation of samples, equipment, instruments, the setup of experiments and the procedure.

3.2. Materials and Methods

In this section, the materials used and the methods of tests that were carried out are explained.

3.2.1. Materials

The materials used were commercial which went through the following stage: first grinding raw materials (Nile clay, silica sand, weather granite, kaolin, sodium silica, S.T.P.P, master mix) and then sprayed and kept in silos and pressed using (SAMI PH3590 PRESS) and pressed from 160 to 180 Bar, and then dried and it passed the glaze line which consists of (quartz, feldspar, Ball clay, I. Kaolin, Engobe frit-19, matt frit-13, opaque frit-188, Transparent frit-575, Zirconium silicate ($ZrSiO_4$), calcined alumina, transparent printing-106, transparent printing-1000, reactive printing powder-606), four rectangular specimens A, B, C and D were made with length of 2 cm, width 1 cm and thickness 2 mm, see Figure 3.1.

Three of these specimens (B, C and D) were exposed Nd: YAG laser with 60 W output power at continuous mode, with different irradiation times (3, 4 and 5) min and one specimen was left without treatment (A) as reference.

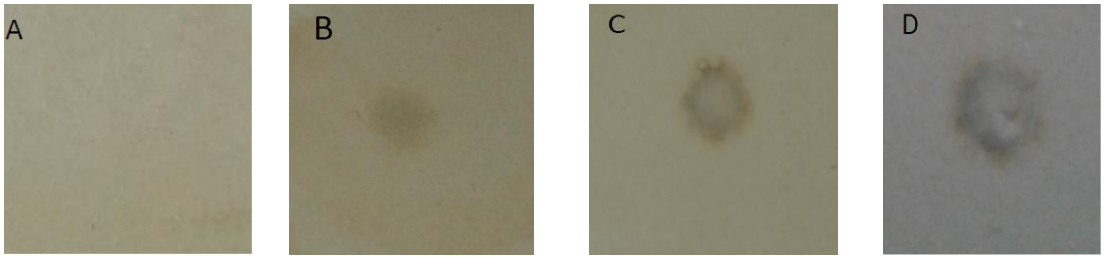

Figure 3.1: specimens Images of Zirconium Silicate Surface After Nd: YAG Laser Irradiation (60 W): (A) 0 min Irradiation Duration, (B) 3 min Irradiation Duration, (C) 4 min Irradiation Duration and (D) 5 min Irradiation Duration

3.2.2. Apparatus

Several device were used to perform the test

3.2.2.1. Nd: YAG Laser

The laser used in the irradiation process (Figure 3.2) was Nd: YAG laser system (Dornier Medilas fiber to 5100) from institute of laser-(SUST).

Figure 3.2: Nd_YAG Laser device

3.2.2.2. Hardness Device

The hardness of the irradiated and non-irradiated specimens (Figure 3.3) was tested using the Vickers Hardness (ZHU250, ZWICK/ROELL, GERMANY, 2015) from Materials Research Center, Khartoum, Sudan.

Figure 3.3: Hardness device

3.2.2.3. Scanning Electron Microscope

An analysis of the morphology of the irradiated and non-irradiated specimens (Figure 3.4) was tested using electron microscopy (SEM), including a local analysis of the chemical composition (EDX) (TESCAN, Vega III/Czech Republic) from General Directorate Petroleum Laboratories Research & Studies – Ministry of Petroleum, Khartoum, Sudan.

Figure 3.4: Scanning Electron Microscopedevice

3.2.2.4. FTIR Spectrometer

The chemical groups presented in the irradiated sites in the specimens and a non-irradiated specimen (Figure 3.5) was tested using Fourier transform infrared spectrometer **(**Satellite FTIR 5000**)** From the Chemistry Lab at the University of Sudan, Khartoum, Sudan.

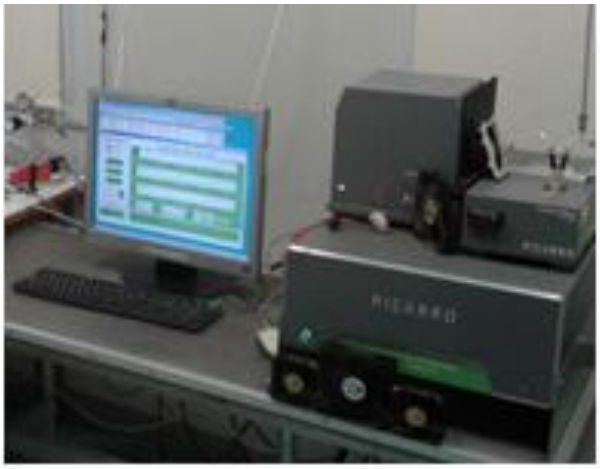

Figure 3.5: FTIR Spectrometer

3.2.2.5. UV-Visible Spectrometer

the effect of laser irradiation on the absorbance of the irradiated specimens and the non-irradiated specimens (Figure 3.6) was tested using Ultraviolet Visible spectrometer (Jasco-670 UV-Visible spectrometer) from institute of laser-(SUST).

Figure 3.6: UV-Visible Spectrometer

3.2.3. Method

3.2.3.1. Laser Irradiation

An Nd: YAG laser system (Dornier Medilas fiber to 5100) operating at a wavelength of 1064 nm with continuous mode was used to irradiate specimen. Specimens were placed one by one and the Nd: YAG laser beam was projected

perpendicular to the surface of the specimens. The distance from the laser window to the specimen surface was approximately 7 mm. The laser power was 60 W and laser irradiation treatments were carried out without any water spray (dry laser). All tests and characterizations were done on the exposed area in the samples.

3.2.3.2. Hardness and Tensile strength Tests

The hardness of the irradiated and non-irradiated specimens were tested using the Vickers Hardness method (ZHU250, ZWICK/ROELL, GERMANY, 2015). The principle of the Vickers Hardness method is similar to the Brinell method. The Vickers indenter is a 136 degrees square-based diamond pyramid. The impression, produced by the Vickers indenter is clearer than the impression of Brinell indenter; therefore, this method is more accurate. The load, varying from 1kgf to 120 kgf, is usually applied for 30 seconds. The Vickers number (HV) is calculated by the following formula (3.1):

$$HV = 1.854 \times F / D^2 \quad (3.1)$$

Where: F ≡ applied load/kg; D ≡ length of the impression diagonal/ mm

The length of the impression diagonal is measured using a microscope, which is usually an integral part of the Vickers Tester.

Tensile strength was calculated using the following equation (3.2):

$$Ts = 3.45 \times HB \quad (3.2)$$

3.2.3.3. SEM and EDX Analysis

An analysis of the morphology of the surface layer was made for the irradiated and non-irradiated specimens using electron microscopy (SEM), including a local analysis of the chemical composition (EDX). The surface morphology of the impact sites was examined using a scanning electron microscope (TESCAN, Vega III/Czech Republic). The analysis of characteristic X-rays (EDX analysis) emitted from the sample gives more quantitative elemental information. Such X-ray analysis can be confined to analytical volumes as small as one cubic micron.

3.2.3.4. FTIR Spectroscopy

The chemical groups presented in the irradiated sites in the specimens and non-irradiated specimens were determined by the Fourier transform infrared spectrometer. FTIR samples were prepared to scan by mixed them with dry potassium bromide powder, then applying sufficient pressure. FTIR spectra of the samples were carried out in the wavenumber varying from 400 cm−1 to 4000 cm−1 using (FTIR) spectrometer (Satellite FTIR 5000).

3.2.3.5. UV-vis spectroscopy

To study the effect of laser irradiation on the absorbance of the irradiated specimens and the non-irradiated specimens an aqueous suspension of the zirconium silicate was carried out using a Jasco-670 UV-Visible spectrometer.

CHAPTER FOUR

RESULTE AND DISCUSSION

4.1. Introduction

In this chapter, the obtained results are presented in tables, figures and spectroscopic drawings. The obtained results were discussed, as well as the conclusions written and also the recommendations for future studies.

4.2. Results and Discussions

The photo-thermal effect of the irradiation of zirconium silicate specimens with Nd: YAG laser at 1064 nm wavelength and 60 W output power with continuous mode for different durations generates heat witch caused in the following results:

4.2.1. Hardness and Tensile Strength Results

The results of irradiation with Nd: YAG laser (power 60 W) at different duration time (0, 3, 4 and 5) minutes on the zirconium silicate specimens' hardness were listed in Table 4.1. It shows that the hardness of the irradiated samples was obviously increased. A considerable increasing in hardness with increasing irradiation time from 3 to 5 minutes was found; it changed at a constant irradiation time at one minute. It increased about one third (37.5%) at irradiation time three

minutes, it increased the half (50%) at four minutes and about two thirds (62.5%) at five minutes.

Table 4.1 Hardness results for untreated zirconium silicate sample (A) and zirconia treated with Nd: YAG laser specimens (B, C and D)

Sample	Hardness/ HV=1.8544 F/D^2	Hardness/HB	Hardness changes/HB	Change %
A	8.1	8	0	0
B	10.5	11	3	37.5
C	11.7	12	4	50
D	12.6	13	5	62.5

The results of irradiation on the zirconium silicate specimens' tensile strength were listed in Table 4.2. It was calculated by applying the following equation:

$$Ts = 3.45 \times HB$$

Table 4.2 Tensile strength results for untreated zirconium silicate sample (A) and zirconia treated with Nd: YAG laser specimens (B, C and D)

Sample	Hardness/ HB	Tensile strength/ MPa	Tensile strength changes/ MPa	Change %
A	8	27.6	0	0
B	11	37.95	10.35	27.27
C	12	41.4	13.8	33.33

D	13	44.85	17.25	38.46

The experimental data presented in Tables 1 and 2 show that, in all experiments, a linear correlation between hardness or tensile strength and laser irradiation time was detected.

Figure 4.1 A) depict the linear correlation between hardness and irradiation time. While Figure 4.1 B) depict the linear correlation between hardness change and irradiation time.

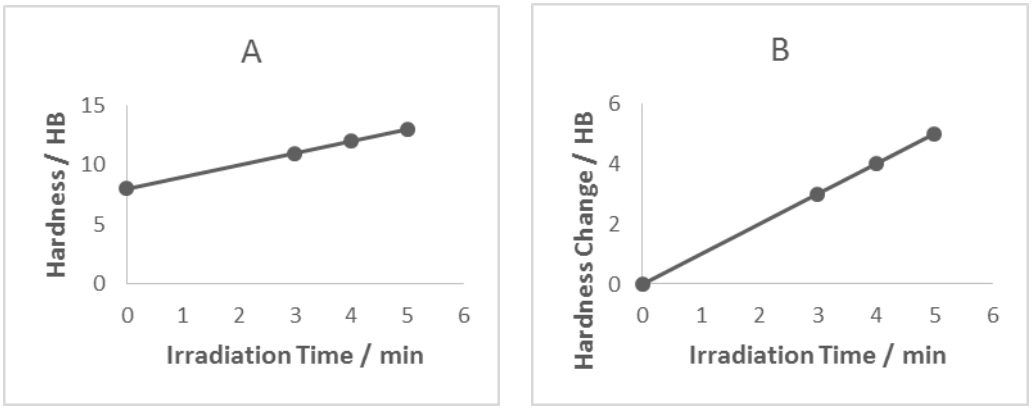

Figure 4.1 Effect of irradiation time on zirconium silicate samples' A) hardness B) change in hardness

Figure 4.2 depict A) depict the linear correlation between tensile strength and irradiation time, While Figure 4.2 B) depict the linear correlation between tensile strength change and irradiation time.

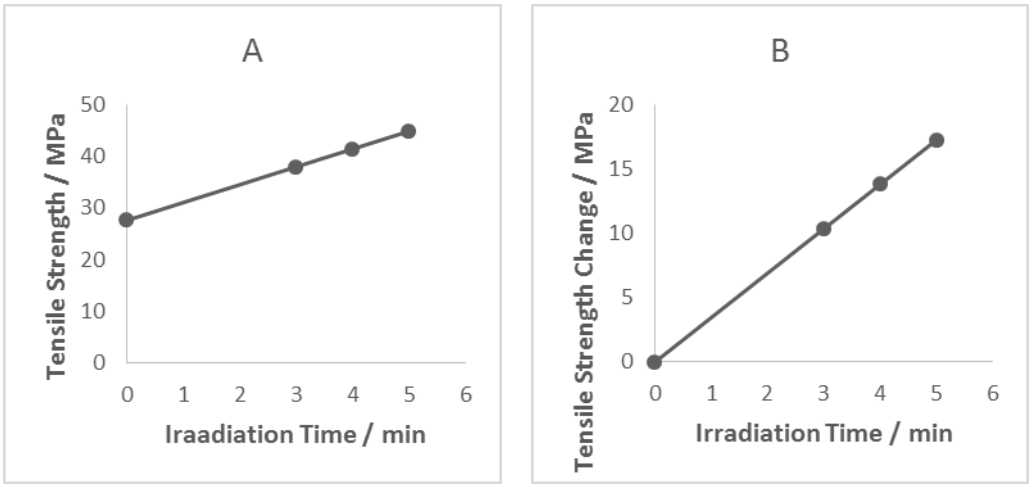

Figure 4.2 Effect of irradiation time on zirconium silicate samples' A) tensile strength B) tensile strength change

Graphs in Figures 4.1 and 4.2 presented that extending irradiation time can induce higher hardness of the ceramics.

4.2.2. SEM Results

The SEM images (50 μm scale) of the zirconium silicate surface obtained with irradiation duration equal to 3, 4 and 5 min are shown in Figure 4.3. It shows that different irradiation times of irradiation induced different surface morphology.

The SEM images of Nd: YAG laser-irradiated sites in specimens (B), (C) and (D) showed a nonhomogeneous rough sites with some irregularities and holes compared to non-irradiated specimen (A). This sites showed the formation of microstructures in the yielded dimples and grooves. There is no thermal damaging effects, like burning, melting, and cracks, was found. No microcracks were observed proving that the irradiation process does not cause material defect.

It can be observed that they revealed morphology changed from a roughness site (Figure 4.3B) to a smooth site (Figure 4.3D), depending on the irradiation duration, which is meaning solidification process occurring on the specimens' surfaces in all accumulated irradiation duration. This result is agreeable with the previous linear correlation between hardness and tensile strength with laser irradiation time.

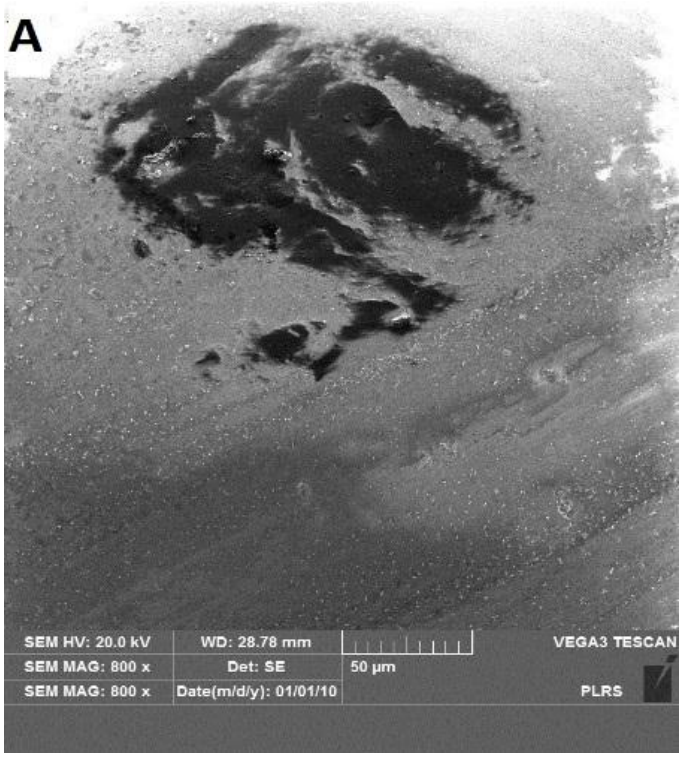
A
SEM HV: 20.0 kV
WD: 28.78 mm
VEGA3 TESCAN
SEM MAG: 800 x
Det: SE
50 µm
SEM MAG: 800 x
Date(m/d/y): 01/01/10
PLRS

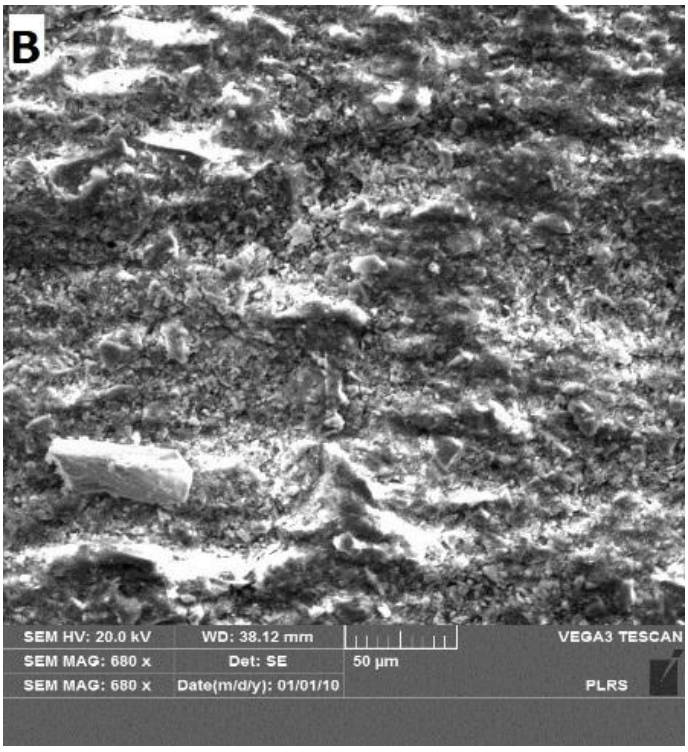
B
SEM HV: 20.0 kV
WD: 38.12 mm
VEGA3 TESCAN
SEM MAG: 680 x
Det: SE
50 µm
SEM MAG: 680 x
Date(m/d/y): 01/01/10
PLRS

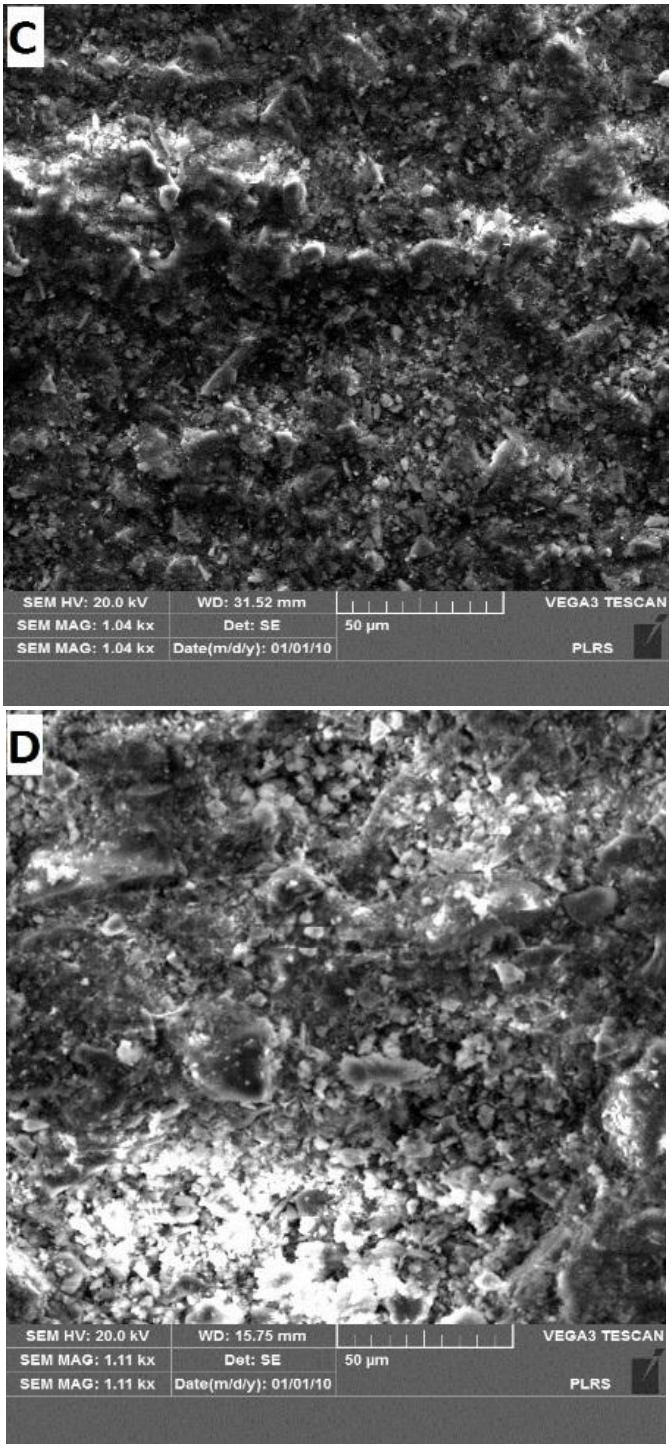

Figure 4.3: SEM Images of Zirconium Silicate Surface After Nd: YAG Laser Irradiation (60 W): (A) 0 min Irradiation Duration, (B) 3 min Irradiation Duration, (C) 4 min Irradiation Duration and (D) 5 min Irradiation Duration

4.2.3. EDX Results

The EDX spectra shown in Figure 4.4 giving the elemental analysis data of the samples before and after laser irradiation treatment (with 4 and 5 minutes). The presence of the same elements is coincides with the results from laser irradiated and non-irradiated specimens, which mean that laser irradiation do not change the chemical surface composition of ceramics. EDX spectra show that the zirconium and silicon have the highest peaks compared to the other elements as shown in Table 4.3.

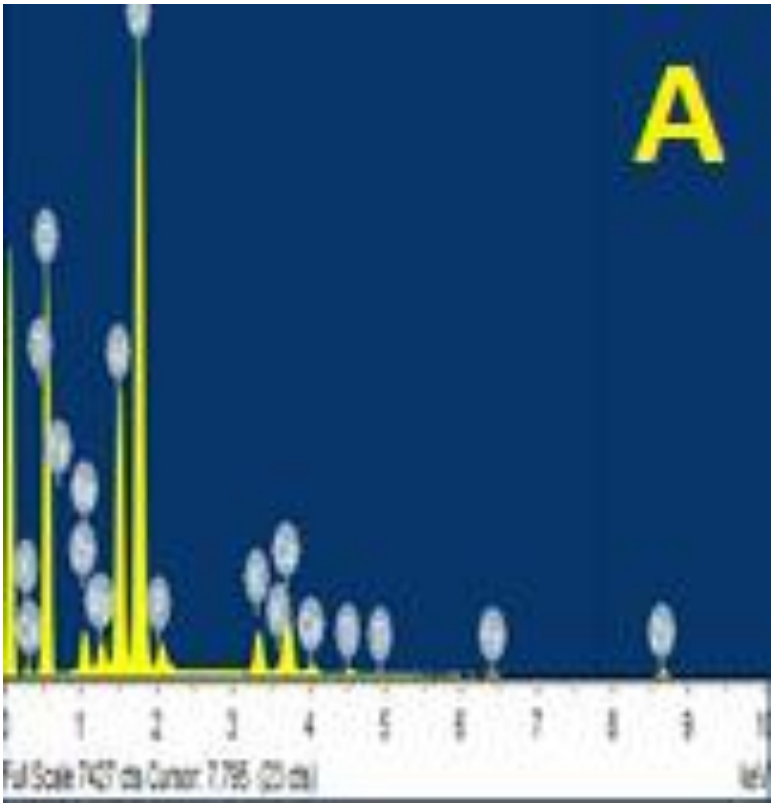
A
1
2
3
4
5
6
7
8
9

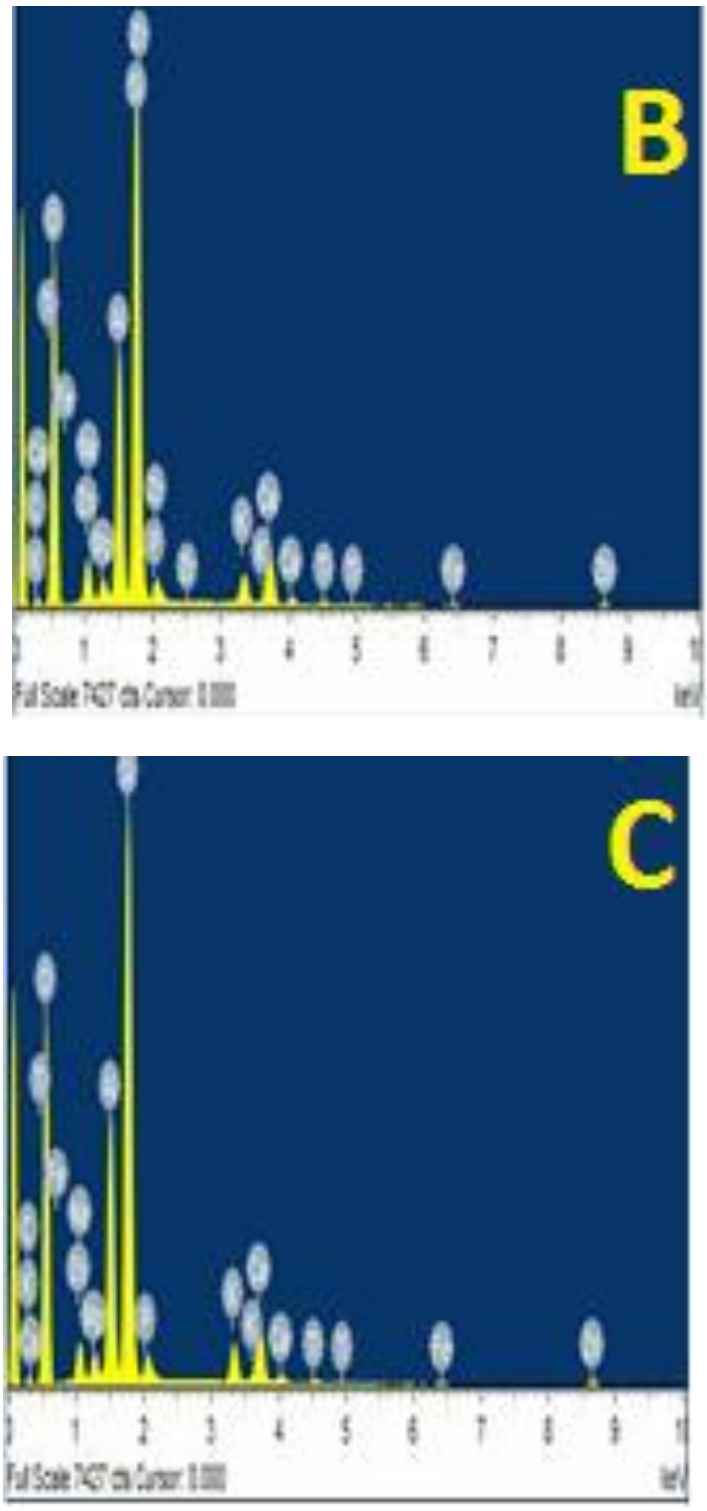

Figure 4.4: EDX spectra of zirconium silicate (A) before, B) and C) after Nd: YAG laser irradiation (60 W): 0, 4 and 5 min irradiation duration respectively

Table 4.3 EDX results of zirconium silicate sample (A) before, sample B) and samples C) after Nd: YAG laser irradiation (60 W): 0, 4 and 5 min irradiation duration respectively

Element	Sample A		Sample C		Sample D	
	Weight%	Atomic%	Weight%	Atomic%	Weight%	Atomic%
C K	0	0	2.95	4.87	6.20	10.04
O K	54.14	68.64	54.31	67.30	51.70	62.82
Na K	1.70	1.50	1.61	1.39	1.88	1.59
Mg K	1.09	0.91	0.89	0.73	0.81	0.65
Al K	9.51	7.15	8.94	6.57	8.78	6.32
Si K	23.59	17.03	21.25	15.00	21.19	14.67
P K	1.24	0.81	0.64	0.41	1.21	0.76
K K	2.22	1.15	1.76	0.89	1.75	0.87
Ca K	3.71	1.88	3.45	1.71	3.23	1.57
Ti K	0.26	0.11	0.23	0.09	0	0
Fe K	0.57	0.21	0.29	0.10	0.27	0.09
Zn K	1.97	0.61	1.73	0.52	1.63	0.49
Zr L	0	0	1.96	0.43	0	0
Pt M	0	0	0	0	1.34	0.13
Totals	100.00		100.00		100.00	

4.2.4. UV-vis Spectroscopy Results

The UV-vis spectroscopy spectra of the four samples are shown in Figure 4.5. Decreased absorbance was observed in the laser-irradiated samples in the visible and near infrared range (350-800 nm). When comparing non-irradiated sample with each of the laser irradiated samples, non-irradiated sample always showed higher absorbance. The process of laser irradiation presented effect in transmittance of the zirconium silicate.

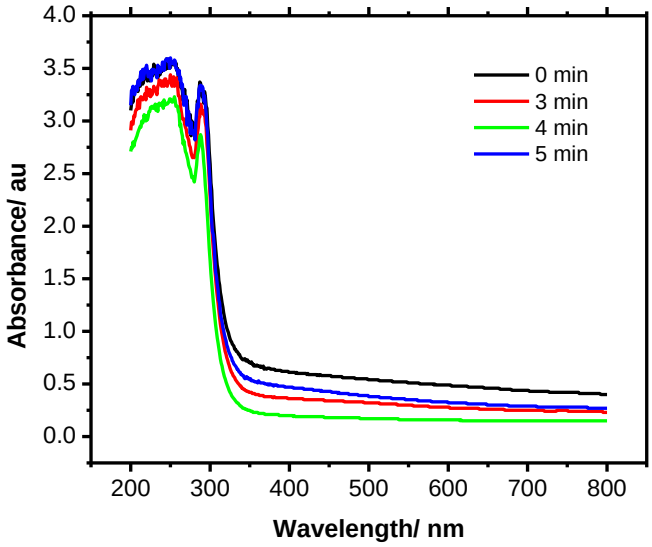

Figure 4.5: UV spectra of zirconium silicate specimens before and after laser irradiation

4.2.5. FTIR Results

The FTIR spectra of zirconium silicate specimens a) before laser irradiation and b, c and d) and after laser irradiation are shown in Figure 4.6 and it was tabled in Table 4.4. The spectra showed hydroxyl groups (O-H) in deferent positions; the bands around 3696 cm-1 and 3620 cm-1 assigned outer and inner hydroxyl stretching vibration (Müller, et al., 2014; Kumararaja, et al., 2017), a broad band centered on 3442 cm-1 was due to the interlayer and intralayer H-bonded O-H stretching (Kumararaja, et al., 2017). Peak in the region of 3431 cm-1 also denotes the presence of hydroxyl groups (O-H) (Balan, et al., 2019).

Spectra also shwoed other functional groups such as amide, clay minerals, and silica. The amide A band (associated with N–H stretching) positions at 3423 cm-1 (Riaz, et al., 2018). The peak identified at 1025 cm-1 that correspond to the C−O stretching (Balan, et al., 2019). The 1033 cm-1 band is attributed to the Si-O stretching vibration (Vijayaragavan, et al., 2013). Clay minerals (Diopside) are characterized by the presence of 920 cm-1 (De Benedetto, et al., 2002). The band at 787 cm-1 is attributed to the stretching vibrations of Te-O bonds trigonal pyramids (Upender, and Prasad, 2017). The symmetrical bending vibration of the amorphous silica Si–O (quartz) group found at 695 cm-1 (Saikia, et al., 2008), this quartz with small particle size, improves mechanical strength of the ceramic bodies. The band at about 536-538 cm-1 is attributed to the coupling between the

O-Si-O bending vibration and the K-O stretching vibration (Theodosoglou, et al., 2010). Al–O–Si and Si–O–Si bending vibrations produced the bands at 538 and 470 cm-1, respectively (Yin, et al., 2019).

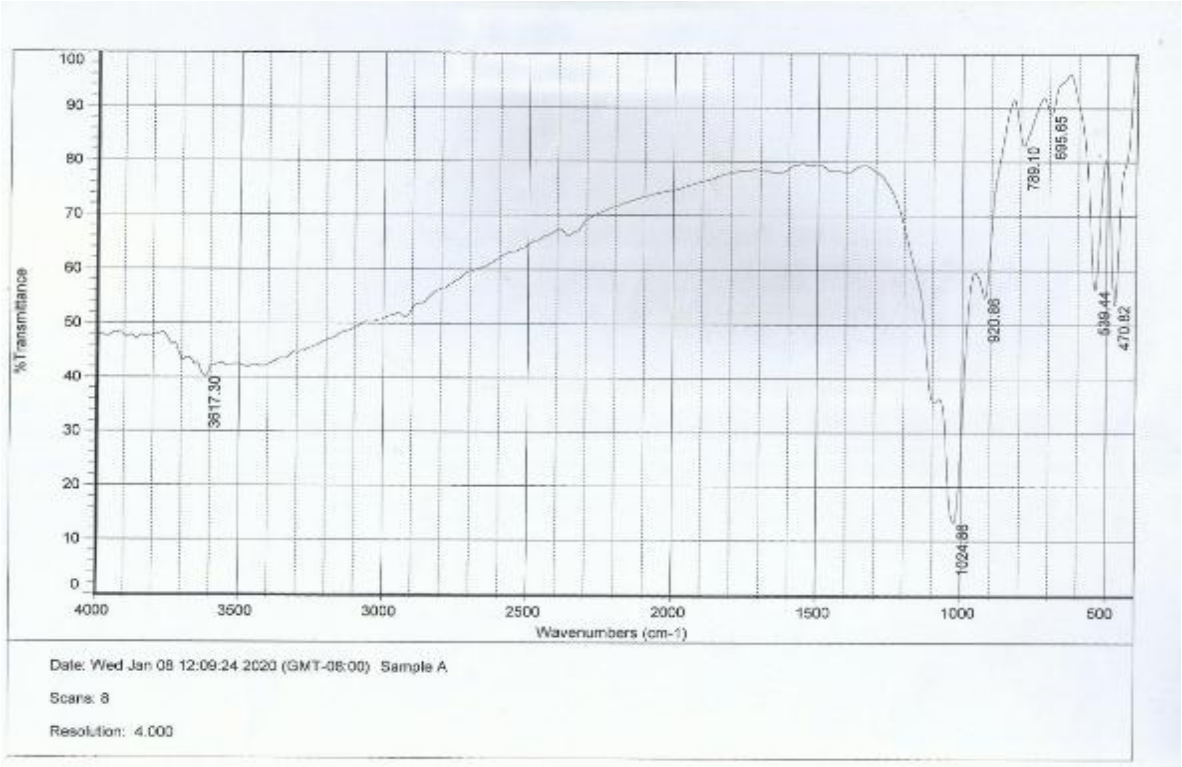

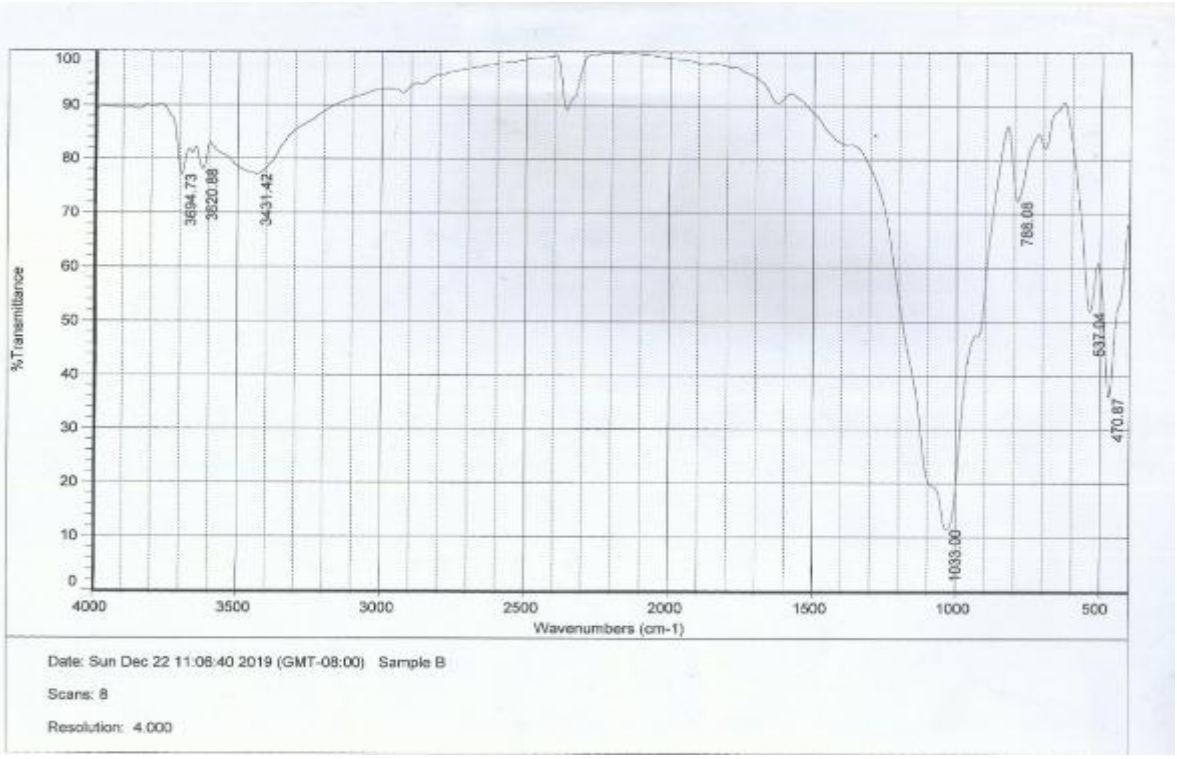
%Transmittance
100
90
80
70
60
50
40
30
20
10
0
4000
3500
3000
2500
2000
1500
1000
500
Wavenumbers (cm-1)
3694.73
3620.88
3431.42
788.08
537.04
470.87
1033.00
Date: Sun Dec 22 11:08:40 2019 (GMT-08:00) Sample B
Scans: 8
Resolution: 4.000

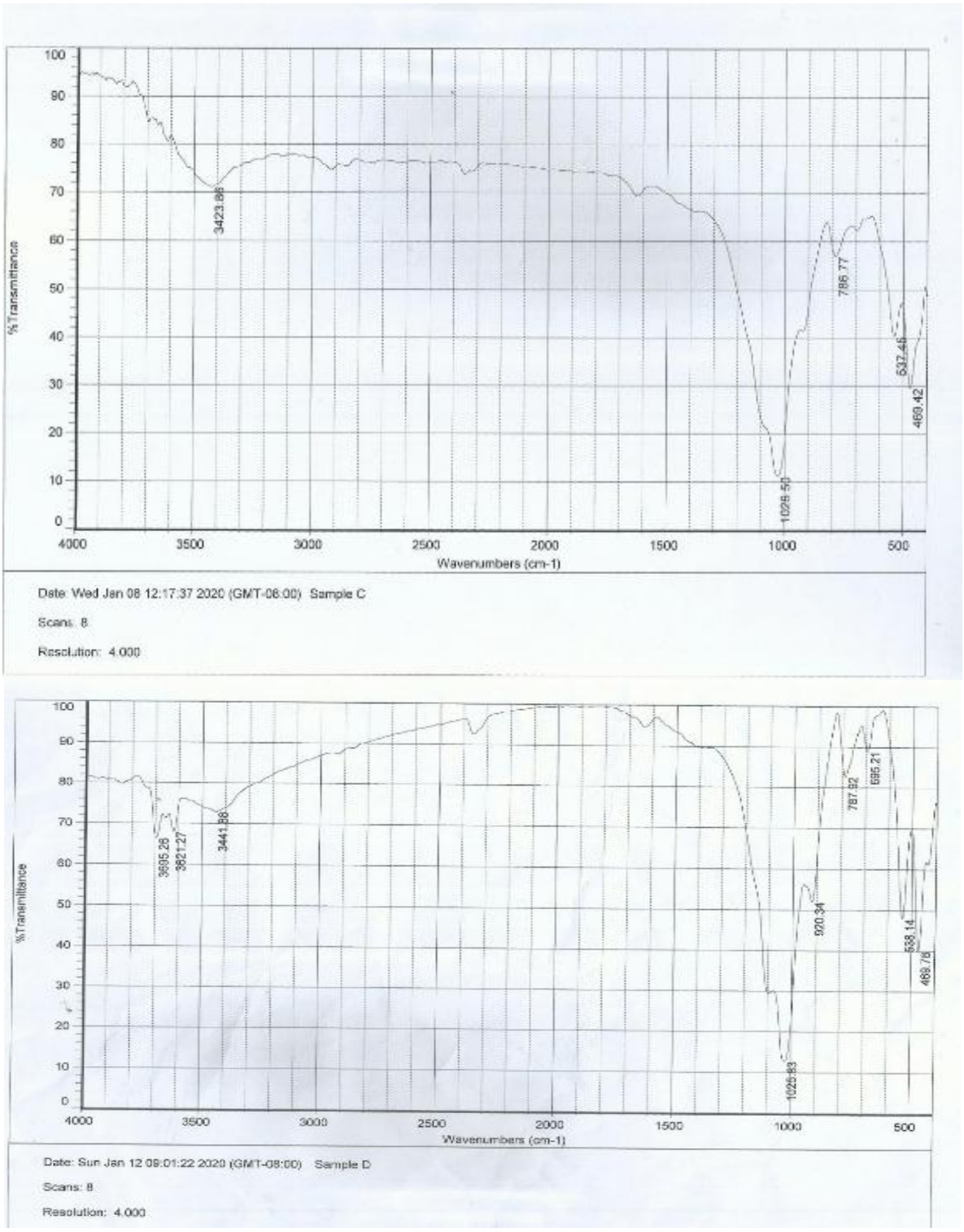

Figure 4.6: FTIR spectra of zirconium silicate specimens a) before laser irradiation b,c and d) and after laser irradiation

Table 4.4. The main structural shifts observed in IR

Assignment	Characteristic Absorption (cm^{-1})				Reference
	Sample A	Sample B	Sample C	Sample D	
Inner surface-OH vibrations.	3695.26	-	3694.73	-	Müller, *et al.*, 2014
O-H stretching inner hydroxyl group	3621.27	3617.30	3620.88	-	Kumararaja, *et al.*, 2017
O-H stretching	3441.88	-	-	-	Kumararaja, *et al.*, 2017
hydroxyl groups (O-H)	-	-	3431.42	-	Balan, *et al.*, 2019
N–H stretching	-	-	-	3423.86	Riaz, *et al.*, 2018
C−O stretching	1025.83	1024.88	-	1026.50	Balan, *et al.*, 2019
Si-O stretching vibration	-	-	1033.00	-	Vijayaragavan, *et al.*, 2013
Diopside	920.34	920.86	-	-	De Benedetto, *et al.*, 2002
Te-O bonds	787.92	-	788.08	786.77	Upender, and Prasad, 2017
Amorphous silica Si–O (quartz)	695.21	-	-	-	Saikia, *et al.*, 2008
coupling between O-Si-O bending and K-O stretching vibrations	538.14	539.44	537.04	537.45	Theodosoglou, *et al.*, 2010
Si–O–Si bending vibrations	469.78	470.82	470.87	469.42	Yin, *et al.*, 2019

4.3. Conclusion

The photo thermal effect of the irradiation of zirconium silicate specimens with Nd: YAG laser at 1064 nm wavelength and 60 W output power with continuous mode for different durations was investigated. The hardness test show that Nd: YAG laser irradiation with (60 W) can increase the hardness of zirconium silicate ceramics. SEM images demonstrate the formation of microstructures, smoother surface and solidification process occurring confirming the hardness results. FTIR spectra denotes the presence of amorphous silica Si-O with small-sized particle, which enhances mechanical strength of the zirconium silicate. Moreover, EDX results reveal that laser irradiation does not modify the chemical composition of ceramics surface. In addition, UV-vis spectra showed more transmittance of irradiated zirconium silicate specimens compared to the non-irradiated specimens. Nd: YAG laser irradiation with (60 W) can increase the hardness of zirconium silicate ceramics. In summary, the experimental results revealed a linear correlation between laser irradiation duration and hardness, tensile strength and surface solidification, without causing material defect.

4.4. Recommendations

- This work obtained that high-powered lasers could be used to enhance the properties of ceramic construction materials and industrial chemicals, have been looking for markets for their transparent ceramics.

- For future studies; researchers could investigate the crystal structure of the irradiated ceramic.

References

Ahmed, M.M., Abdelrahman, A.H., Mohieldin, E. and Yagoub, S.O., 2014. Effect of Diode Laser 810nm in Hardness of Dental Ceramic. *Optics and Photonics Journal*, 2014.

Al Humira Elseir Gorashe Ahmmed, A. and Marouf, A.S., 2017. Effect of Pulsed He-Ne Laser Irradiation on Bee Honey Physicochemical Properties. *The Saudi Journal of Life Sciences (SJLS)*.

Amna O.B Malik and Marouf, A.A., 2018. Comparison of the Effects of Laser Pasteurization and Heat Pasteurization on The Cow's Milk, *Haya: The Saudi Journal of Life Sciences*.

Balan, V., Mihai, C.T., Cojocaru, F.D., Uritu, C.M., Dodi, G., Botezat, D. and Gardikiotis, I., 2019. Vibrational spectroscopy fingerprinting in medicine: From molecular to clinical practice. *Materials*.

Braga, F.J., Marques, R.F. and GUASTALDI, A.C., 2014. Surface modification of Ti dental implants by Nd: YVO_4 laser irradiation. *Applied Surface Science*.

De Benedetto, G.E., Laviano, R., Sabbatini, L. and Zambonin, P.G., 2002. Infrared spectroscopy in the mineralogical characterization of ancient pottery. *Journal of Cultural Heritage*.

Dubey, A.K. and Yadava, V., 2008. Laser beam machining—a review. *International Journal of Machine Tools and Manufacture*.

El-Ghany, O.S.A. and Sherief, A.H., 2016. Zirconia based ceramics, some clinical and biological aspects. *Future dental journal*.

Fiechtner, G.J., King, G.B., Laurendeau, N.M. and Lytle, F.E., 1992. Measurements of atomic sodium in flames by asynchronous optical sampling: theory and experiment. *Applied optics*.

Fotakis, C., Anglos, D., Zafiropulos, V., Georgiou, S. and Tornari, V., 2006. *Lasers in the preservation of cultural heritage: principles and applications*. CRC Press.

Garcia-Sanz, V., Paredes-Gallardo, V., Mendoza-Yero, O., Carbonell-Leal, M., Albaladejo, A., Montiel-Company, J.M. and Bellot-Arcis, C., 2018. The effects of lasers on bond strength to ceramic materials: A systematic review and meta-analysis. *PloS one*.

Garvie, R.C., Hannink, R.H. and Pascoe, R.T., 1975. Ceramic steel?. *Nature*.

Gawbah, M.A.P., Elbadawi, A.A., Alsabah, Y.A., Orsod, M.U. and Marouf, A.A., 2018. Characterization of the Crystal Structure of Sesame Seed Cake Burned by Nd: YAG Laser. *Journal of Materials Science and Chemical Engineering*.

Gawbah, M.A.P., Marouf, A.A., Alsabah, Y.A., Orsod, M.U. and Elbadawi, A.A., 2017. Synthesis of Silica, Silicon Carbide and Carbon from Wheat Bran and Converting Its Crystal Structure Using Nd: YAG Laser. *Future*.

Geiger, Greg. 2018. *Introduction To Ceramics*. American Ceramic Society.

Haimid, M.A., Marouf, A.A. and Abdalla, M.D., 2019 a. Helium-Neon Laser Effects on Human Whole Blood by Spectroscopy In vitro Study. *Asian Journal of Physical and Chemical Sciences*, pp.1-6. doi:10.9734/AJOPACS/2019/46214

Haimid, M.A., Marouf, A.A. and Abdalla, M.D., 2019 b. In vitro UV-Visible and FTIR Spectroscopy Study of Low Power He-Ne Laser Irradiation on Human Blood. *Asian Journal of Research and Reviews in Physics*.

Kumararaja, P., Manjaiah, K.M., Datta, S.C. and Sarkar, B., 2017. Remediation of metal contaminated soil by aluminium pillared bentonite: synthesis, characterisation, equilibrium study and plant growth experiment. *Applied Clay Science*.

Lee, W.B.E., Burakov, B.E. and Ojovan, M.I., 2010. *Crystalline Materials For Actinide Immobilisation* (Vol. 1). World Scientific.

Marouf, A. and Sara, I.E., 2018. Monitoring pH During Pasteurization of Raw Cow's Milk using Nd: YAG Laser. *International Journal of Advanced Research in Physical Science (IJARPS)*.

Marouf, A.A., Abdalah, S.F., Abdulrahman, W.S. and Al Naimee, K., 2014. The Role of Photonic Processed Si Surface in Architecture Engineering. *Study of Civil Engineering and Architecture*.

Marouf, A.A., Khairallah Y. A., 2019. Photoemission Spectra of Sound Tooth and Those of Different Carious Stages. *European Journal of Biophysics.*

McColm, I.J., 2013. *Ceramic hardness*. Springer Science & Business Media.

Müller, C.M., Pejcic, B., Esteban, L., Delle Piane, C., Raven, M. and Mizaikoff, B., 2014. Infrared attenuated total reflectance spectroscopy: an innovative strategy for analyzing mineral components in energy relevant systems. *Scientific reports.*

Petrie, G. and Toth, C.K., 2008. Introduction to laser ranging, profiling, and scanning. *Topographic laser ranging and scanning: Principles and processing*.

Pich, O., Franzen, R., Gutknecht, N. and Wolfart, S., 2015. Laser treatment of dental ceramic/cement layers: transmitted energy, temperature effects and surface characterisation. *Lasers in medical science*.

Radousky, H.B., 2006. *Science & Technology Review September 2006* (No. UCRL- TR-52000-06-9). Lawrence Livermore National Lab.(LLNL), Livermore, CA (United States).

Renk, K.F., 2012. *Basics of laser physics*. Berlin: Springer Berlin Heidelberg.

Riaz, T., Zeeshan, R., Zarif, F., Ilyas, K., Muhammad, N., Safi, S.Z., Rahim, A., Rizvi, S.A. and Rehman, I.U., 2018. FTIR analysis of natural and synthetic collagen. *Applied Spectroscopy Reviews*.

Saikia, B.J., Parthasarathy, G. and Sarmah, N.C., 2008. Fourier transform infrared spectroscopic estimation of crystallinity in SiO_2 based rocks. *Bulletin of Materials Science.*

Sanusi, S., Seow, W.K. and Walsh, L.J., 2012. Effects of Er: YAG laser on surface morphology of dental restorative materials. *Journal of Physical Science.*

Seuba, J., Deville, S., Guizard, C. and Stevenson, A.J., 2016. Mechanical properties and failure behavior of unidirectional porous ceramics. *Scientific reports*.

Siegman, A.E., 1986. Lasers university science books. *Mill Valley, CA.*

Theodosoglou, E., Koroneos, A., Soldatos, T., Zorba, T. and Paraskevopoulos, K.M., 2010. Comparative Fourier transform infrared and X-ray powder diffraction analysis of naturally occurred K-feldspars. *Bulletin of the Geological Society of Greece.*

Thys, M. and Desmet, E., 2011. *Laser beams: theory, properties and applications*. Nova Science Publ.

Türkmen, C., Sazak, H. and Günday, M., 2006. Effects of the Nd: YAG laser, air-abrasion, and acid-etchant on filling materials. *Journal of oral rehabilitation.*

Upender, G. and Prasad, M., 2017. Raman, FTIR, thermal and optical properties of TeO2-Nb2O5-B2O3-V2O5 quaternary glass system. *Journal of Taibah University for Science*.

Vijayaragavan, R., Mullainathan, S., Balachandramohan, M., Krishnamoorthy, N., Nithiyanantham, S., Murugesan, S. and Vanathi, V., 2013. Mineralogical characterization studies on unburnt ceramic product made from rock residue additives by FT-IR spectroscopic technique. *In International Journal of Modern Physics*.

Wachtman Jr, J.B., 1999. Ceramic innovations in the 20 th century. *American Ceramic Society, Inc, 735 Ceramic Place, Westerville, OH 43081, USA.*

Yariv, A., 1989. Quantum well semiconductor lasers are taking over. *IEEE Circuits and Devices Magazine*.

Yin, Y., Yin, H., Wu, Z., Qi, C., Tian, H., Zhang, W., Hu, Z. and Feng, L., 2019. Characterization of Coals and Coal Ashes with High Si Content Using Combined Second-Derivative Infrared Spectroscopy and Raman Spectroscopy. *Crystals*.